THE GERONTOLOGICAL SOCIETY OF AMERICA®

OXFORD

Original Article

BDA-410 Treatment Reduces Body Weight and Fat Content by Enhancing Lipolysis in Sedentary Senescent Mice

Andrea S. Pereyra,[1,2] Zhong-Min Wang,[1] Maria Laura Messi,[1] Tan Zhang,[1,3] Hanzhi Wu,[4] Thomas C. Register,[5,6] Elizabeth Forbes,[5] Nelmi O. Devarie-Baez,[4] Daniel Clark Files,[1,7] Martin C. Abba,[8] Cristina Furdui,[4] and Osvaldo Delbono[1,3]

[1]Department of Internal Medicine, Section on Gerontology and Geriatric Medicine, Wake Forest School of Medicine, Winston-Salem, North Carolina. [2]Biochemistry Research Institute of La Plata (INIBIOLP)/CONICET, School of Medicine, National University of La Plata, Buenos Aires, Argentina. [3]J Paul Sticht Center on Aging, Wake Forest School of Medicine, Winston-Salem, North Carolina. [4]Molecular Medicine and Translational Science, [5]Department of Neurobiology and Anatomy, [6]Department of Pathology, Section on Comparative Medicine, and [7]Pulmonary and Critical Care Allergy and Immunology, Wake Forest School of Medicine, Winston-Salem, North Carolina. [8]Basic and Applied Immunological Research Center (CINIBA), School of Medicine, Universidad Nacional de La Plata, Buenos Aires, Argentina.

Address correspondence to Osvaldo Delbono, MD, PhD, Department of Internal Medicine, Section on Gerontology and Geriatric Medicine, Wake Forest School of Medicine, Medical Center Boulevard, Winston-Salem, NC 27157. E-mail: odelbono@wakehealth.edu

Abstract

Loss of muscle mass and force with age leads to fall risk, mobility impairment, and reduced quality of life. This article shows that BDA-410, a calpain inhibitor, induced loss of body weight and fat but not lean mass or skeletal muscle proteins in a cohort of sedentary 23-month-old mice. Food and water intake and locomotor activity were not modified, whereas BDA-410 treatment decreased intramyocellular lipid and perigonadal fat, increased serum nonesterified fatty acids, and upregulated the genes mediating lipolysis and oxidation, lean phenotype, muscle contraction, muscle transcription regulation, and oxidative stress response. This finding is consistent with our recent report that lipid accumulation in skeletal myofibers is significantly correlated with slower fiber-contraction kinetics and diminished power in obese older adult mice. A proteomic analysis and immunoblot showed downregulation of the phosphatase PPP1R12B, which increases phosphorylated myosin half-life and modulates the calcium sensitivity of the contractile apparatus. This study demonstrates that BDA-410 exerts a beneficial effect on skeletal muscle contractility through new, alternative mechanisms, including enhanced lipolysis, upregulation of "lean phenotype-related genes," downregulation of the PP1R12B phosphatase, and enhanced excitation–contraction coupling. This single compound holds promise for treating age-dependent decline in muscle composition and strength.

Keywords: Skeletal muscle—Aging—Calpain—Body fat—Sarcopenia

Skeletal muscle plays a role in systemic aging and constitutes an independent determinant of life span (1). Loss of muscle mass and force with age, termed sarcopenia, leads to fall risk, mobility impairment, and reduced quality of life (2). We discovered that decreased expression of the voltage-gated calcium channel α1 subunit (Ca$_v$1.1) accounts for excitation–contraction uncoupling and force decline with aging (3–5). We also reported that increased expression of Ca$_v$β1a subunit contributes to skeletal muscle weakness by decreasing levels of Ca$_v$1.1 protein without interfering with transcription of its encoding gene, *Cacna1s* (6). These and other mechanisms underlying skeletal muscle impairment with aging have been reviewed (7,8).

Recently, we reported that troponin T3 (TnT3) regulates *Cacna1s* transcription and Ca$_v$1.1 expression by binding a consensus sequence at the *Cacna1s* promoter region. Furthermore, endogenous cleavage of TnT3 accounts for decreased Ca$_v$1.1 expression with aging (9,10). Detailed analysis of the TnT3-*Cacna1s* interaction showed that the TnT3 endogenous cleavage site in muscle in vivo is compatible with calpain activity, and BDA-410, a synthetic cyclopropenone derivative that specifically and reversibly inhibits cysteine proteases such as calpains (11), stabilizes nuclear TnT3 integrity in skeletal muscle from old mice in vivo. We also found that calpain inhibition does not modify overall levels of the main motor and regulatory proteins or

fiber type in fast and slow muscles from old mice. We discovered that inhibiting calpain by oral BDA-410 administration rescued $Ca_v1.1$ protein levels in old sedentary mice and enhanced muscle excitation–contraction coupling and force generation in old mice (9,10,12).

Here, we report that, compared to control vehicle-treated mice, BDA-410-treated mice experienced significant decrease in body weight. Because changes in body weight occurred in a cohort of mice that exhibited improved skeletal muscle force, we examined whether BDA-410 activates metabolic pathways involved in protein and/or lipid metabolism and their potential to increase muscle function. Because most relevant proteins involved in force generation did not change with BDA-410 treatment (10), we hypothesized that loss in body fat accounts for the observed loss in body weight and enhanced muscle force. White adipose tissue (WAT) is involved in pathways regulating life span, age-related diseases, inflammation, and metabolic dysfunction, and its removal from visceral depots enhances insulin sensitivity and extends life span in laboratory rodents (13). Because we reported that lipid accumulation in skeletal myofibers significantly correlates with slower fiber-contraction kinetics and diminished power in obese older adults (14), we propose that BDA-410-induced fat loss contributes to enhanced force generation in sedentary senescent mice.

This study shows that BDA-410 may exert a beneficial effect on skeletal muscle contractility through new, alternative mechanisms to those recently proposed (10), including enhanced lipolysis, upregulation of "lean phenotype-related genes," and downregulation of the PP1R12B phosphatase, which increases phosphorylated myosin half-life and modulates calcium sensitivity of the contractile apparatus. A single compound that combines all these major positive effects has great potential in treating age-dependent decline in muscle composition and strength.

Materials and Methods

Animals

Twenty-three-month-old female C57BL/6 mice from the Charles River-NIA colony were used for this and our previous report (10). They were housed in a pathogen-free area at Wake Forest School of Medicine (WFSM), four per cage, at 20–23°C, with a 12:12-h dark–light cycle, and ad-libitum access to food and water. Mouse handling and procedures followed a protocol approved by the WFSM Animal Care and Use Committee.

BDA-410 Administration Protocol

The calpain inhibitor BDA-410, (2S)-N-(1S)-1-[(S)-hydroxy(3-oxo-2-phenyl-1-cyclopropen-1-yl)methyl]-2-methylpropyl-2-benzenesulfonylamino-4-methylpentanamide, is a cyclopropenone derivative, synthesized and kindly provided by Mitsubishi Tanabe Pharma Corporation (Yokohama, Japan). Two groups of 23-month-old mice received either 1% Tween 80 in normal saline (vehicle) or BDA-410 dissolved in vehicle at 30 mg/kg/d by gavage for 21 consecutive days. This dose and administration route are reported to lead to a 24 nM plasma concentration and a maximum concentration after per os bolus of ~12 ng/mL (15).

Statistical Analysis

Data were analyzed using SigmaPlot 12.5 (Systat Software, San José, CA) or Prism 6.0a (GraphPad Software, La Jolla, CA). All data are expressed as means ± *SEM*, and reported *p* values are the result of two-sided tests. The alpha level was set at $p < .05$. Student's *t*-test or analysis of variance was used to compare experimental groups where appropriate.

See Supplementary Methods for a detailed description of skeletal muscle collection, measurements of body weight, body composition, food and water intake, spontaneous locomotor activity, microarray data processing and statistical analysis, real-time PCR mRNA analysis, nanoscale liquid chromatography to tandem mass spectrometry, label-free protein quantification using precursor integrity, intramyocellular lipid (IMCL), fiber type and nonesterified fatty acids assay, sodium dodecyl sulfate–polyacrylamide gel electrophoresis, and immunoblotting for PP1R12B phosphatase.

Results

BDA-410 Induced Loss in Body Weight and Fat Content

We treated two groups of 23-month-old female C57BL/6 mice with either 1% Tween 80 dissolved in saline (vehicle group) or 30 mg/kg/d BDA-410 dissolved in vehicle (BDA-410 group) by gavage for 21 consecutive days. At baseline, mice weight did not differ between groups (Figure 1A), but the percent change in body weight between posttreatment and pretreatment was statistically significant (Figure 1B; *p* = .01), because the vehicle-treated group increased, whereas the BDA-410-treated group decreased. To determine whether changes in body composition account for body weight loss with BDA-410 treatment, we measured body fat and lean mass by dual-energy X-ray absorptiometry scanning (Figure 1C). Although the BDA-410 group lost a significant amount (~16%) of body fat, the vehicle-treated mice gained ~8% (*p* = .042). Lean mass (in grams) did not differ between BDA-410- (pre: 20.0±0.44, post: 21.2±0.42; *p* = .1) and vehicle-treated (pre: 20.8±0.43, post: 20.6±0.48; *p* = .365) mice. Figure 1D illustrates dual-energy X-ray absorptiometry scans of a mouse before and after BDA-410 treatment. These results indicate that BDA-410 induces body weight loss by reducing fat content without altering muscle mass (10). We also recorded the weight of perigonadal WAT (Figure 1E), lung, heart, spleen, kidney, and liver (Figure 1G). The loss in fat content is statistically significant only in perigonadal WAT and soleus muscle. Histological measures of lipid droplets (total lipid droplet area, number of lipid droplets, average of each droplet area, and area fraction) in the soleus muscle from BDA-410- and vehicle-treated mice show that, compared to vehicle, BDA-410 significantly decreases IMCL content in both type-1 and type-II fibers (Figure 1F and Table 1). The significant increase of serum nonesterified fatty acids concentration in BDA-410-treated mice compared to vehicle-treated mice (Figure 1G) further supports the conclusion that BDA-410 enhances lipolysis in sedentary senescent mice.

BDA-410 Administration Does Not Modify Food and Water Intake

We also examined whether reductions in calorie or water intake contributed to loss of body fat content or body weight, respectively. Daily food and water intake were recorded for each mouse for 3 consecutive days before and after BDA-410 or vehicle administration and normalized to body weight recorded the same day. Figure 2 shows that BDA-410- and vehicle-treated mice did not differ in absolute (Figure 2A) or normalized-to-body-weight (Figure 2B) food intake and absolute (Figure 2C) or normalized (Figure 2D) water intake. These data indicate that BDA-410 does not alter food or water intake suggesting that changes in body weight and fat were independent of caloric intake.

BDA-410 Does Not Modify Spontaneous Locomotor Activity

As physical activity may result in body weight loss through increased energy expenditure, we examined whether BDA-410 induced

increased mouse activity compared to baseline and the control group. Mice were placed on an open field arena, and their spontaneous activity was recorded continuously for 2–5 minutes in the absence

Figure 1. BDA-410 treatment induced loss of weight and body fat but not lean mass in mice. Baseline (**A**) and change (**B**) in mouse body ($n = 8$ vehicle, $n = 9$ BDA-410; *$p = .01$). (**C**) Change in body fat measured by dual-energy X-ray absorptiometry scans ($n = 8$ vehicle, $n = 9$ BDA-410; *$p = .042$). (**D**) Representative dual-energy X-ray absorptiometry scans of a BDA-410-treated mouse that lost 28% of its body fat. Dotted lines denote the thickness of subcutaneous WAT in the flank ($n = 4$). (**E**) Perigonadal fat weight in BDA-410- ($n = 5$) and vehicle-treated mice ($p < .05$). (**F**) Oil-red-O staining of soleus muscle from BDA-410- and vehicle-treated mice. (**G**) Lung, heart, spleen, kidney, liver, and soleus muscle weight and serum nonesterified fatty acids concentration in BDA-410- ($n = 5$) and vehicle-treated ($n = 5$) mice.

or presence of an object using a computerized tracking system. We computed time spent moving in the empty field (Figure 3A), total distance traveled (Figure 3C), average speed (Figure 3E), and spontaneous maximal speed (Figure 3G) over 3 consecutive days before and immediately after BDA-410 or vehicle treatment. The same parameters were recorded in the presence of an object (Figure 3B, D, and F). Although overall mobility and total travel time tended to be lower in the BDA-410-treated mice than the control, the difference was not statistically significant. Because BDA-410 did not increase spontaneous locomotion, it must induce the leaner phenotype by another mechanism.
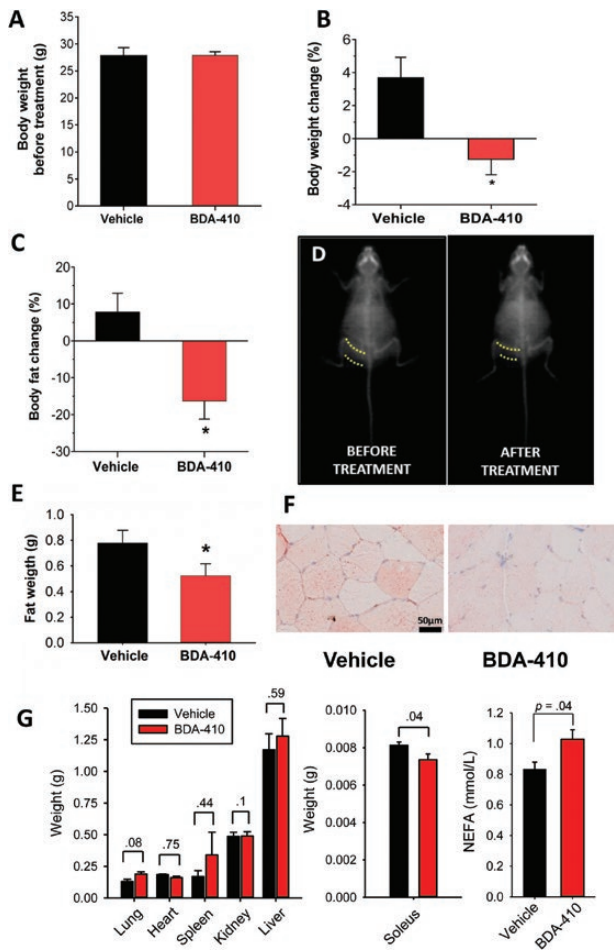
BDA-410 Treatment Reduces IMCL

IMCL data were obtained in 6 mice (3 BDA-410 and 3 vehicle treated), and a total of 335 soleus fibers (160 BDA-410, 175 vehicle) were identified by their lipid droplet characteristics and fiber type, determined by Oil-red-O (Figure 1F) and ATP-ase staining (14). As shown in Table 1, type-I fibers had greater total lipid droplet area and more lipid droplets ($p < .01$) than type-II fibers in both groups, but this difference was more pronounced in the vehicle group. Additionally, total lipid droplet area, number of lipid droplets, average of each droplet area, and area fraction were about twofold greater in both type-I and type-II fibers from the vehicle group compared to the BDA-410 group ($p < .01$). In summary, fibers from the vehicle group showed about a twofold greater area of lipid droplet than fibers from the BDA-410 group, especially in the type-I fibers.

Genes Encoding Mediators of Lipolysis and Fat Oxidation are Upregulated in the Skeletal Muscle of BDA-410-Treated Mice

To understand the mechanism underlying the loss in body weight and fat recorded in BDA-410-treated mice, we examined the gastrocnemius muscle's transcriptome using RNA microarrays in mice treated with BDA-410 or vehicle. The statistical analysis revealed 2,559 differentially expressed transcripts with –2.05- to 9.85-fold change ($p < .05$); specifically, 1,241 genes were upregulated (1.02- to 9.84-fold change), whereas 1,318 were downregulated (–1.02- to –2.05-fold change). A volcano plot shows the general distribution of these transcripts according to statistical significance (y-axis, p value) and fold change (x-axis, means difference; Figure 4A). Gene ontology annotation of 106 genes with a change larger than 1.5-fold revealed major clustering around the following biological processes: lipid metabolism, the peroxisome proliferator-activated receptor (PPAR)-adiponectin pathway, the insulin-like growth factor 1 pathway, response to oxidative stress, and cell aging (Figure 4B).

Table 1. Intramyocellular lipids in BDA-410- and vehicle-treated mice

	BDA-410		Vehicle	
	Type I (102 fibers)	Type II (58 fibers)	Type I (108 fibers)	Type II (67 fibers)
Droplet area (µm²)	198 ± 9.4[a]	72 ± 5.8	357 ± 28[a,b]	130 ± 5.9[b]
Number of lipid droplets	124 ± 4.5[a]	48 ± 3.1	214 ± 9[a,b]	88 ± 5.6[b]
Average of each droplet area (µm²)	1.3 ± 0.05	1.1 ± 0.05	1.5 ± 0.04[a,b]	1.4 ± 0.07[b]
Area fraction (%)	6.1 ± 0.32[a]	2.7 ± 0.09	9.1 ± 0.17[a,b]	4.6 ± 0.45[b]

Data are mean ± SEM.

Total number of muscle fibers analyzed: 335.

[a]Significantly different than type-II fiber type within group treatment.

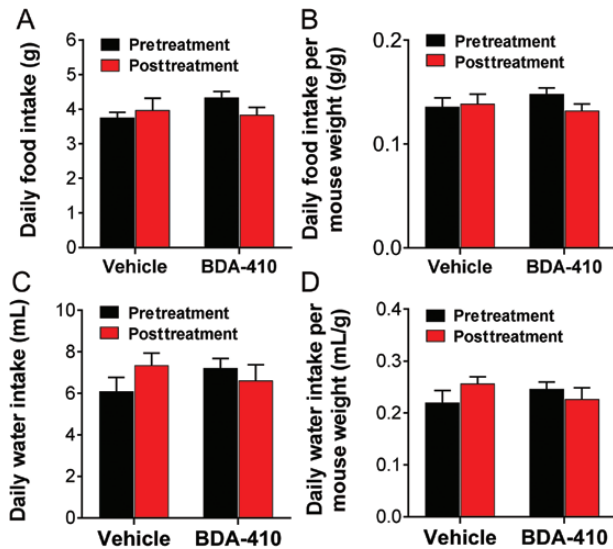[b]Significantly different than corresponding fiber type of BDA-410 group.

Figure 2. BDA-410 did not modify food and water intake. Daily food (**A**) and water (**B**) intake recorded for each mouse 3 consecutive days before and after treatment and normalized to mouse weight (**C** and **D**) (n = 5 mice for BDA-410-treated mice and n = 4 mice for the vehicle-treated group).
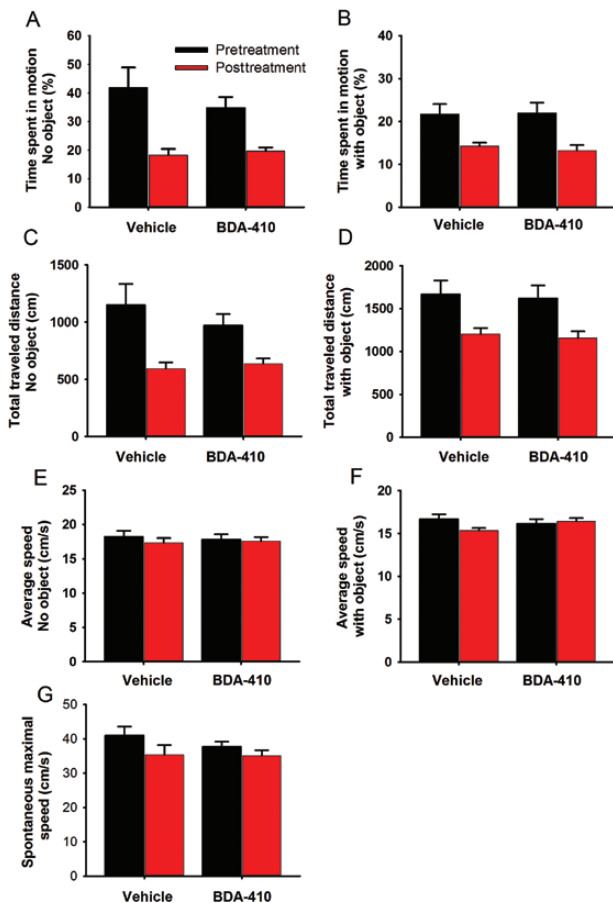

Figure 3. BDA-410 did not modify spontaneous locomotor activity. Mouse mobility tested in an open field arena in the absence (**A, C, E, G**) or presence (**B, D, F**) of an object. Mice treated with BDA-410 (n = 5) or vehicle (n = 4) were examined for time spent in motion (**A** and **B**); percent of the trial spent moving (**C**); total traveled distance (**D**); average speed (**E** and **F**); and spontaneous maximal speed (**G**).

To define the molecular pathways modified by BDA-410, we searched for relevant genes among those differentially expressed. Supplementary Table 1 lists selected transcripts, and a heat map represents the expression level of each sample for both mouse groups (Figure 4C). We confirmed upregulation of *Adipoq*, *Dgat1*, *Angptl4*, *Fabp4*, and *Ppard* gene transcripts by qPCR. Values for relative expression post- and pre-BDA-410 treatment were 8.4 ± 1.7, 1.9 ± 0.23, 4.1 ± 0.62, 3.2 ± 0.46, and 1.5 ± 0.33, respectively.

Figure 4D shows the functional connections between these 24 differentially expressed genes in (Figure 4C) using the STRING$_{10}$ database. The most significantly upregulated genes were *Adipoq*, *Angptl4*, *Fabp4*, *Retnla*, *Dgat1*, *Acsl3*, *Cdh13*, and *Ppard* (see Supplementary Table 1 and Figure 5), which codify for adiponectin (ADIPOQ), angiopoietin-like 4 (ANGPTL4), fatty acid binding protein 4 (FABP4), resistin-like alpha (RETNLA), diacylglycerol O-acyltransferase 1 (DGAT1), acyl-CoA synthetase long-chain family member 3, T-cadherin, and peroxisome proliferator-activated receptor delta (PPARδ) proteins, respectively. In contrast, known negative modulators of metabolic pathways such as *Nrip1* (nuclear receptor interacting protein 1 or RIP140) and *Ppargc1b* (peroxisome proliferator-activated receptor-γ coactivator-1β [PGC-1β]) were downregulated, contributing to increased transcription of the *Ppard* gene and its downstream effectors, such as ANGPTL4, which activate lipolysis.

Apart from voluntary physical activity, skeletal muscle metabolism and endocrine function have a significant impact on whole-body metabolic homeostasis by producing and secreting molecules with paracrine and endocrine function, termed myokines. In BDA-410 treated mice, mRNA was upregulated for five myokine genes: *Adipoq* (+9.85-fold change; p = .023), *Ifi27l2a* (+3.20-fold change; p = .045), *Angptl4* (+2.59-fold change; p = .007), *Fabp4* (+2.46-fold change; p = .016), and *Retnla* (+2.25-fold change; p = .021; Supplementary Table 1). These genes may mediate body fat loss in BDA-treated mice by stimulating muscle-derived lipolysis and inhibiting adipocyte differentiation (see the following sections). Note that *Adipoq*, *Ucp3* (mitochondrial uncoupling protein 3; +1.28-fold change; p = .040), *Dgat1* (+1.45-fold change; p = .041), and *Ppard*, which are significantly upregulated in the skeletal muscle of BDA-410-treated mice (Supplementary Table 1), are directly associated with a lean phenotype.

BDA-410 Upregulates Genes Associated With Muscle Contraction Regulation, Calcium Homeostasis, Excitation–Contraction Coupling, and Actin Filament Dynamics

BDA-410 increased expression of genes involved in (a) skeletal muscle structure and function, including *Igf1* (insulin-like growth factor 1; +1.70-fold change; p = .034), *Igfbp3* (insulin-like growth factor 1 binding protein 3; +1.94-fold change; p = .010), and *Igfbp4* (insulin-like growth factor 1 binding protein 4; +1.95-fold change; p = .023); (b) intracellular calcium homeostasis and excitation-contraction coupling: *Camk2d* (calcium/calmodulin-dependent protein kinase II delta; +1.46-fold change; p = .018), *Csrp3* (cysteine- and glycine-rich protein 3/muscle LIM protein; +2.50-fold change; p = .038), and *Dnm2* (dynamin-2; –1.07-fold change; p = .038); and (c) actin filament dynamics: *Gsn* (gelsolin; +1.53-fold change; p = .034; Supplementary Table 1).

BDA-410 Induces Overexpression of Genes Associated With Transcription Regulation

Gene expression involves finely tuned regulation by factors that modulate the timing and frequency of DNA transcription. In mice, BDA-410
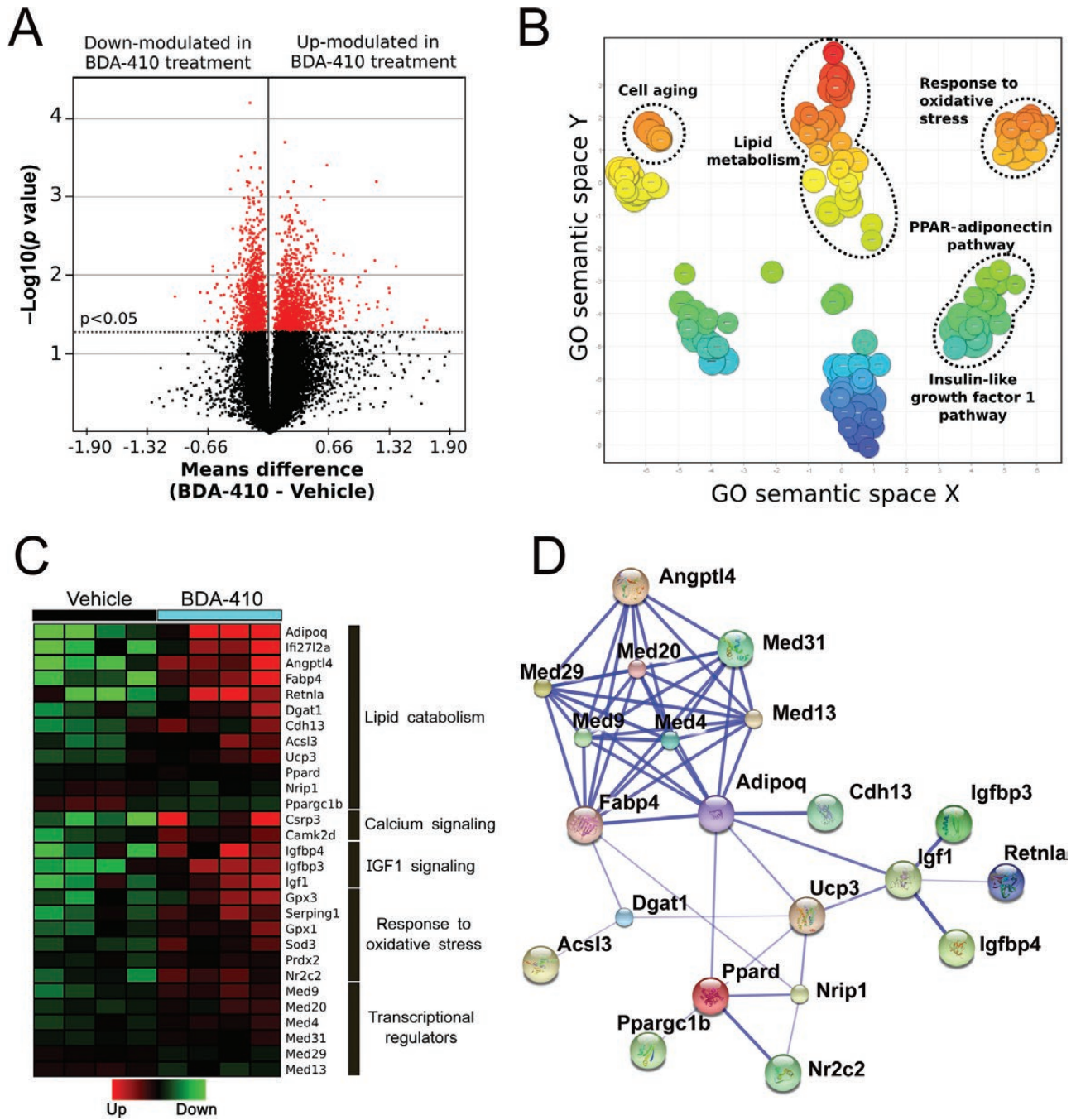
Figure 4. Effects of BDA-410 on skeletal muscle gene expression. (**A**) Volcano plot representing differentially expressed genes in the gastrocnemius muscle of BDA-410- and vehicle-treated mice. Dots represent gene transcripts. The red dots represent those that displayed high statistical significance (y-axis; $p < .05$). The x-axis shows the mean difference between the BDA-410 ($n = 4$) and control ($n = 4$) groups; it measures the magnitude of change in expression levels. (**B**) Gene ontology (GO) classification. Scatterplot of significant biological pathways ($p < .05$), including genes showing over a 1.5-fold change with treatment. (**C**) Supervised clustering analysis of differentially expressed genes. The heat map shows differential expression of 24 selected genes in the skeletal muscle from BDA-410- and vehicle-treated mice. Fold change values are in Supplementary Table 1. (**D**) Protein–protein interactions among the 24 selected, differentially expressed genes. Thicker lines represent stronger associations.

increases a group of transcription factors generically known as mediator complex (MED), including *Med4*, *Med9*, *Med20*, and *Med31*. The transcription factor *Nr2c2* (nuclear receptor subfamily 2, group C, member 2) is also upregulated, whereas *Med13*, *Med29*, *Nrip1*, and *Ppargc1b* are downregulated compared to skeletal muscle from vehicle-treated mice (Supplementary Table 1). These transcription factors have been reported to regulate *Ppard*, *Angptl4*, and *Adipoq* gene expression (Figure 5).

BDA-410 Upregulates Genes Associated With Oxidative Stress Response

By ontology analysis, we found that transcripts related to oxidative stress response form a cluster in BDA-410-treated compared to vehicle-treated mice. Upregulated genes in this cluster include: *Gpx3* (glutathione peroxidase 3), *Serping1* (serine [or cysteine] peptidase inhibitor, clade G, member 1), *Gpx1* (glutathione peroxidase 1),
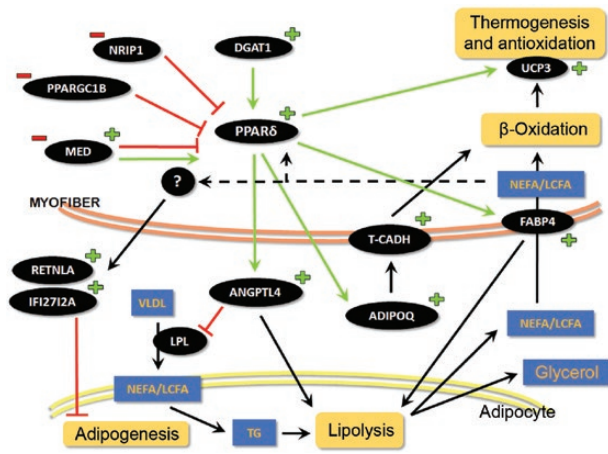
Figure 5. Schematic representation of differentially expressed genes in the skeletal muscle of old, sedentary C57BL/6 mice after BDA-410 treatment. This scheme shows several signaling cascades and the corresponding metabolic pathways involved in skeletal muscle-adipose tissue crosstalk. The plus (+) and minus (–) signs represent upregulated and downregulated genes, respectively, in BDA-treated mice compared to vehicle-treated mice. Arrows show positive regulation, whereas truncated lines represent an inhibitory action or effect. TG = triglycerides; NEFA/LCFA = nonesterified fatty acids/long-chain fatty acids; VLD = very-low-density lipoprotein.

Sod3 (superoxide dismutase 3), and *Prdx2* (peroxiredoxin 2; Supplementary Table 1).

BDA-410 Treatment Downregulates PPP1R12B Muscle Phosphatase

Because calpains have many intracellular targets, we analyzed the protein expression profile of whole protein extractions from soleus muscle of BDA-410- and vehicle-treated mice (*n* = 3 muscles from 3 mice per group) by nanoscale liquid chromatography coupled to tandem mass spectrometry. Data analysis showed significant differences between groups for proteins with few known connections with the previously discussed pathways, except for protein phosphatase 1 regulatory subunit 12B (PPP1R12B; protein 47 in Supplementary Table 2), which plays a crucial role in muscle force development by modulating the calcium sensitivity of the contractile apparatus. We confirmed by immunoblot that PPP1R12B was downregulated in the BDA-410 compared to the vehicle group (Figure 6A and B).

Discussion

The morbidity and mortality rates of several aging-related diseases correlate with functional capacity, metabolic demand, and muscle mass, and skeletal muscle metabolic status as well as body weight and composition influence muscle contraction efficiency (16–18). The work reported here shows that BDA-410, a known calpain inhibitor, induces loss of body weight and fat but not lean mass or skeletal muscle proteins in sedentary senescent female mice independently of food and water intake and spontaneous locomotor activity. BDA-410 treatment upregulated genes mediating lipolysis and fat oxidation, lean phenotype, muscle contraction, muscle transcriptional regulation, and oxidative stress responses. In addition, an unbiased protein screening and immunoblot analysis showed downregulation of the phosphatase PPP1R12B.
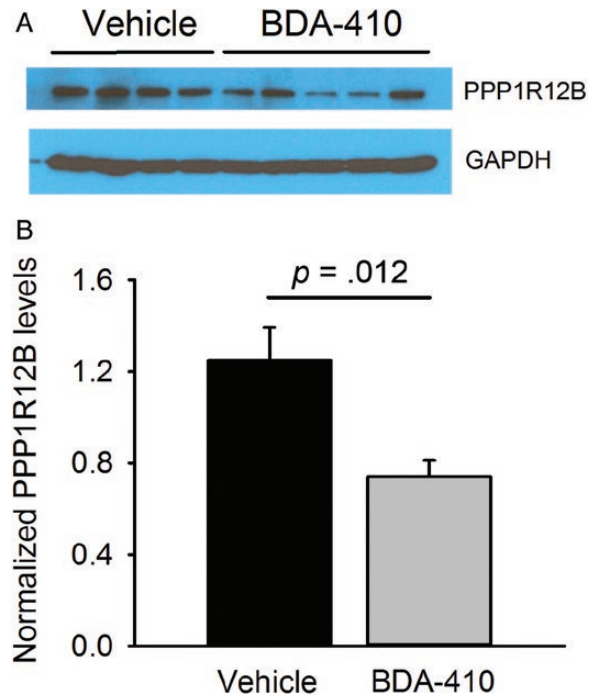

Figure 6. PPP1R12B protein levels decrease in the skeletal muscle of old mice after BDA-410 treatment. (**A**) Representative PPP1R12B and GAPDH immunoblots in gastrocnemius muscles from BDA-410-treated (*n* = 5) and vehicle-treated (*n* = 4) groups. (**B**) PPP1R12B expression levels normalized to GAPDH (**p* = .024).

Body Weight, Body Composition, and Lipolysis

Our data indicate that systemic administration of BDA-410 to old C57BL/6 mice evokes differential expression of many genes involved in lipid metabolism, energy homeostasis, and muscle-adipose tissue crosstalk. BDA-410 significantly induced transcription of key muscle-derived metabolic modulator genes, such as *Angptl4*, *Adipoq*, *Ppard*, and *Retnla*, as well as their cellular receptors and downstream effectors. These molecules are responsible for promoting lipolysis, blocking adipogenesis, and increasing fatty acid uptake and oxidation by peripheral tissues (19,20). Figure 5 shows a scheme of these pathways and their interaction. The *Ppard* gene encodes PPARδ, the main isoform in skeletal muscle. PPARδ is thought to be a key coordinator of fatty acid oxidation and energy uncoupling in both adipocytes and myocytes (21), and it controls fatty acid transport into the muscle, beta-oxidation, and mitochondrial respiration (22,23). Specific overexpression of PPARδ in mouse skeletal muscle increased FABP3 and uncoupling proteins (UCP) expression and reduced body fat content by decreasing the size of adipose cells (24).

Here, we show that BDA-410 downregulates the *Nrip1* and *Ppargc1b* genes, thus contributing to increased *Ppard* expression. It differentially regulates several members of the mediator complex, upregulating *Med9*, *Med20*, *Med4*, and *Med31* and downregulating *Med29* and *Med13* compared to control. PPARδ positively regulates the *Angptl4* gene, which codifies for angiopoietin-like 4 protein, which the skeletal muscle secretes into the blood stream, where it acts as a myokine, modulating adiposity by inhibiting lipoprotein-lipase and enhancing intracellular lipolysis in WAT (25). Additionally, circulating levels of ANGPTL4 negatively correlate with body weight and body fat content with no changes in calorie intake or physical activity (26). During increased lipolysis, circulating free fatty acids (FFAs) stimulate skeletal muscle to synthesize and secrete fatty acid

binding proteins, especially FABP4. Exposing C2C12 muscle cells to PPARβ/δ agonist increases FABP expression and lipid catabolism (27). PPARδ increases *Acsl3*, which facilitates β-oxidation, thermogenesis, and antioxidation.

Besides increasing lipolysis, BDA-410 may reduce body fat content by inhibiting or blocking adipogenesis and adipocyte differentiation. We show here that BDA-410 significantly increased the expression of two potential myokines with anti-adipogenic properties, *Retnla* and *Ifi27l2a*. *Retnla* codifies for small, cysteine-rich, secreted proteins termed resistin-like alpha (RETNLA), which inhibit adipocyte differentiation (28). They are downregulated in a mouse model of obesity (29) and exert an "atheroprotective cytokine" effect that lowers cholesterol specifically during hyperlipidemia states (30). We speculate that upregulation of *Rentla* levels is an adaptive reaction to increased FFAs in the circulation. Increased *Ifi27l2a* expression might reduce body fat by inhibiting adipogenesis.

BDA-410 and Lean Phenotype-Related Genes

Upregulation of *Ppard*, *Adipoq*, *Ucp3*, and *Dgat1* has been directly associated with body fat and weight loss (31). *Dgat1* codifies for diacylglycerol O-acyltransferase 1, an endoplasmic reticulum-based enzyme involved in triglyceride and retinol synthesis. Increased *Dgat1* expression is responsible for the so-called "athletes' paradox" where both FFA oxidation and triglyceride storage increase in skeletal muscle (32). Mitochondrial UCP are also involved in fatty acid oxidation in skeletal muscle. UCP3 is codified by the *Ucp3* gene, which is positively regulated by PPARδ (22). It seems to be activated by FFAs and reactive oxygen species, and even mild overexpression of UCP3 in skeletal muscle can increase energy expenditure and decrease body weight (31). Here, we report that both genes, *Dgat1* and *Ucp3*, are upregulated in skeletal muscle after administering BDA-410 to old mice, possibly contributing to the observed lean phenotype.

BDA-410 and Oxidative Response

A side effect of increased lipolysis and hyperlipidemia is increased reactive oxygen species production in tissues with elevated FFA uptake and oxidation. In skeletal muscle, the main species are superoxide anion and nitric oxide, which can modulate several cellular functions and have deleterious effects (33). As expected, to protect the cell during increased reactive oxygen species production, many elements of oxidative stress response are activated, including superoxide dismutase (SOD), peroxiredoxin (PRDX), and glutathione peroxidase (GPX). As BDA-410 upregulated the *Sod3*, *Prdx2*, *Gpx1*, and *Gpx3* genes, we hypothesize that the protective response to reactive oxygen species could be triggered by an increased supply of FFAs to the skeletal muscle.

Myosin Phosphorylation and Muscle Contraction Force

BDA-410 successfully attenuated pathologic phenotypes in several mouse models of disease, including models of Alzheimer's disease, aortic aneurism, sickle-cell disease, malaria, spinocerebellar ataxia type 3, and an *α-klotho knockout* mouse model of premature and accelerated aging (15,34–38). However, the effects of BDA-410 in aging mouse skeletal muscle have only recently been explored (10).

We demonstrated that oral administration of BDA-410 to aging C57BL/6 mice inhibited calpain activity in the skeletal muscle and enhanced contraction force in soleus muscle with no change in muscle mass or fiber type composition. This improvement in muscle performance is related to Ca$_v$1.1 upregulation, as TnT3 fragmentation decreases along with CT-TnT3 repression of the *Cacna1s* promoter (10). Here, we found that BDA-410 downregulated PPP1R12B, a key positive regulatory subunit of the myosin phosphatase 1 catalytic subunit delta, which is highly expressed in skeletal muscle (39). It enhances myosin dephosphorylation and reduces calcium sensitivity to promote myofilament relaxation (40). Although PPP1R12B has not yet been reported as a calpain substrate, its leucine-enriched region can be targeted and cleaved by calpains (41). Therefore, we hypothesized that reduced PPP1R12B levels might increase the half-life of phosphorylated myosin and muscle contraction force, consistent with our previous data showing improved muscle performance after BDA-410 administration (10). Our proteomics data agree with our prior observation that BDA-410 does not modify overall skeletal muscle protein expression (10).

Muscle Force Determinants and Energy Metabolism

Evidence of a link between excitation–contraction coupling and energy metabolism in murine skeletal muscle was recently reported (42). The Ca$_v$1.1 channel can modulate fatty acid uptake and oxidation in the myofiber through calcium influx, CaMKII activation, and NO formation. Mice with a genetically modified Ca$_v$1.1 α1 subunit that blocks calcium permeation gained more body weight and fat mass on a chow diet than control mice, without changes in food intake or activity, suggesting that Ca$_v$1.1-mediated CaMKII activation affects muscle energy expenditure. Considering our previous report on muscle force improvement and the restoration of Ca$_v$1.1 level in old, sedentary mice after BDA-410 administration (10), and that Ca$_v$1.1 also plays a role in excitation-transcription coupling (43,44), we believe that further studies should determine the link between these phenomena and the differential expression of the key lipid metabolism-related genes reported here.

Limitations

We recognize several limitations to our study. First, the proteins encoded by the significantly modified transcripts are not represented in our proteomics analysis, and we do not know whether they change with BDA-410 treatment. Second, our data cannot define whether BDA-410's role in lipid metabolism depends on its recognized role as a calpain inhibitor. Third, despite our robust evidence that BDA-410 administration in aged mice leads to differential gene expression, our results do not clearly identify the event that triggers these changes, probably due to the broad, only partially understood targets of calpain in skeletal muscle. Fourth, because the calpain inhibitor is administered systemically, changes induced in tissues, such as WAT or pancreas, might influence the skeletal muscle response. Fifth, we do not know whether BDA-410 affects macronutrient excretion in feces; however, this has not been reported in previous studies of the effects of BDA-410 on various disease conditions and aging (10,15,34–38,45). Sixth, we cannot say whether the effects of BDA-410 reported here are sex specific; future studies should include male mice. Finally, future studies should determine whether more prolonged administration or a higher BDA-410 concentration produces stronger effects.

Supplementary Material

Please visit the article online at http://gerontologist.oxfordjournals.org/ to view supplementary material.

References

1. Demontis F, Piccirillo R, Goldberg AL, Perrimon N. The influence of skeletal muscle on systemic aging and lifespan. *Aging Cell*. 2013;12:943–949. doi:10.1111/acel.12126

2. Demontis F, Piccirillo R, Goldberg AL, Perrimon N. Mechanisms of skeletal muscle aging: insights from Drosophila and mammalian models. *Dis Model Mech*. 2013;6:1339–1352. doi:10.1242/dmm.012559

3. Renganathan M, Messi ML, Delbono O. Dihydropyridine receptor-ryanodine receptor uncoupling in aged skeletal muscle. *J Membr Biol*. 1997;157:247–253.

4. Renganathan M, Messi ML, Delbono O. Overexpression of IGF-1 exclusively in skeletal muscle prevents age-related decline in the number of dihydropyridine receptors. *J Biol Chem*. 1998;273:28845–28851.

5. Renganathan M, Messi ML, Schwartz R, Delbono O. Overexpression of hIGF-1 exclusively in skeletal muscle increases the number of dihydropyridine receptors in adult transgenic mice. *FEBS Lett*. 1997;417:13–16.

6. Taylor JR, Zheng Z, Wang ZM, Payne AM, Messi ML, Delbono O. Increased CaVbeta1A expression with aging contributes to skeletal muscle weakness. *Aging Cell*. 2009;8:584–594. doi:10.1111/j.1474-9726.2009.00507.x

7. Gonzalez-Freire M, de Cabo R, Studenski SA, Ferrucci L. The neuromuscular junction: aging at the crossroad between nerves and muscle. *Front Aging Neurosci*. 2014;6:208. doi:10.3389/fnagi.2014.00208

8. Delbono O. Expression and regulation of excitation-contraction coupling proteins in aging skeletal muscle. *Curr Aging Sci*. 2011;4:248–259. doi:10.2174/1874609811104030248

9. Zhang T, Birbrair A, Wang ZM, Taylor J, Messi ML, Delbono O. Troponin T nuclear localization and its role in aging skeletal muscle. *Age (Dordr)*. 2013;35:353–370. doi:10.1007/s11357-011-9368-4

10. Zhang T, Pereyra AS, Wang ZM, et al. Calpain inhibition rescues troponin T3 fragmentation, increases Cav1.1, and enhances skeletal muscle force in aging sedentary mice. *Aging Cell*. 2016;15:488–498. doi:10.1111/acel.12453

11. Ando R, Sakaki T, Morinaka Y, et al. Cyclopropenone-containing cysteine proteinase inhibitors. Synthesis and enzyme inhibitory activities. *Bioorg Med Chem*. 1999;7:571–579. doi:10.1016/S0968-0896(99)00007-3

12. Zhang T, Taylor J, Jiang Y, et al. Troponin T3 regulates nuclear localization of the calcium channel Cavß1a subunit in skeletal muscle. *Exp Cell Res*. 2015;336:276–286. doi:10.1016/j.yexcr.2015.05.005

13. Huffman DM, Barzilai N. Role of visceral adipose tissue in aging. *Biochim Biophys Acta*. 2009;1790:1117–1123. doi:10.1016/j.bbagen.2009.01.008

14. Choi SJ, Files DC, Zhang T, et al. Intramyocellular lipid and impaired myofiber contraction in normal weight and obese older adults. *J Gerontol A Biol Sci Med Sci*. 2016;71:557–564. doi:10.1093/gerona/glv169

15. Trinchese F, Fa' M, Liu S, et al. Inhibition of calpains improves memory and synaptic transmission in a mouse model of Alzheimer disease. *J Clin Invest*. 2008;118:2796–2807. doi:10.1172/JCI34254

16. Anker SD, Ponikowski P, Varney S, et al. Wasting as independent risk factor for mortality in chronic heart failure. *Lancet*. 1997;349:1050–1053. doi:10.1016/S0140-6736(96)07015-8

17. Metter EJ, Talbot LA, Schrager M, Conwit R. Skeletal muscle strength as a predictor of all-cause mortality in healthy men. *J Gerontol A Biol Sci Med Sci*. 2002;57:B359–B365.

18. Ruiz JR, Sui X, Lobelo F, et al. Association between muscular strength and mortality in men: prospective cohort study. *BMJ*. 2008;337:a439. doi:10.1136/bmj.a439.

19. Raschke S, Eckel J. Adipo-myokines: two sides of the same coin–mediators of inflammation and mediators of exercise. *Mediators Inflamm*. 2013;2013:320724. doi:10.1155/2013/320724

20. Karstoft K, Pedersen BK. Skeletal muscle as a gene regulatory endocrine organ. *Curr Opin Clin Nutr Metab Care* 2016;19:270–275. doi:10.1097/MCO.0000000000000283

21. Wang YX, Lee CH, Tiep S, et al. Peroxisome-proliferator-activated receptor delta activates fat metabolism to prevent obesity. *Cell*. 2003;113:159–170. doi:10.1016/S0092-8674(03)00269-1

22. Muoio DM, MacLean PS, Lang DB, et al. Fatty acid homeostasis and induction of lipid regulatory genes in skeletal muscles of peroxisome proliferator-activated receptor (PPAR) alpha knock-out mice. Evidence for compensatory regulation by PPAR delta. *J Biol Chem*. 2002;277:26089–26097. doi:10.1074/jbc.M203997200

23. Tanaka T, Yamamoto J, Iwasaki S, et al. Activation of peroxisome proliferator-activated receptor delta induces fatty acid beta-oxidation in skeletal muscle and attenuates metabolic syndrome. *Proc Natl Acad Sci USA*. 2003;100:15924–15929. doi:10.1073/pnas.0306981100

24. Luquet S, Lopez-Soriano J, Holst D, et al. Peroxisome proliferator-activated receptor delta controls muscle development and oxidative capability. *FASEB J*. 2003;17:2299–2301. doi:10.1096/fj.03-0269fje

25. Mandard S, Zandbergen F, van Straten E, et al. The fasting-induced adipose factor/angiopoietin-like protein 4 is physically associated with lipoproteins and governs plasma lipid levels and adiposity. *J Biol Chem*. 2006;281:934–944. doi:10.1074/jbc.M506519200

26. Mattijssen F, Alex S, Swarts HJ, Groen AK, van Schothorst EM, Kersten S. Angptl4 serves as an endogenous inhibitor of intestinal lipid digestion. *Mol Metab*. 2014;3:135–144. doi:10.1016/j.molmet.2013.11.004

27. Holst D, Luquet S, Kristiansen K, Grimaldi PA. Roles of peroxisome proliferator-activated receptors delta and gamma in myoblast transdifferentiation. *Exp Cell Res*. 2003;288:168–176.

28. Blagoev B, Ong SE, Kratchmarova I, Mann M. Temporal analysis of phosphotyrosine-dependent signaling networks by quantitative proteomics. *Nat Biotechnol*. 2004;22:1139–1145. doi:10.1038/nbt1005

29. Moore GB, Chapman H, Holder JC, et al. Differential regulation of adipocytokine mRNAs by rosiglitazone in db/db mice. *Biochem Biophys Res Commun*. 2001;286:735–741. doi:10.1006/bbrc.2001.5460

30. Lee HJ, Bae EJ, Lee SJ. Extracellular a-synuclein—a novel and crucial factor in Lewy body diseases. *Nat Rev Neurol*. 2014;10:92–98. doi:10.1038/nrneurol.2013.275

31. Aguer C, Fiehn O, Seifert EL, et al. Muscle uncoupling protein 3 overexpression mimics endurance training and reduces circulating biomarkers of incomplete ß-oxidation. *FASEB J*. 2013;27:4213–4225. doi:10.1096/fj.13-234302

32. Liu L, Shi X, Choi CS, et al. Paradoxical coupling of triglyceride synthesis and fatty acid oxidation in skeletal muscle overexpressing DGAT1. *Diabetes*. 2009;58:2516–2524. doi:10.2337/db08-1096

33. Powers SK, Duarte J, Kavazis AN, Talbert EE. Reactive oxygen species are signalling molecules for skeletal muscle adaptation. *Exp Physiol*. 2010;95:1–9. doi:10.1113/expphysiol.2009.050526

34. De Franceschi L, Franco RS, Bertoldi M, et al. Pharmacological inhibition of calpain-1 prevents red cell dehydration and reduces Gardos channel activity in a mouse model of sickle cell disease. *FASEB J*. 2013;27:750–759. doi:10.1096/fj.12-217836

35. Li X, Chen H, Jeong JJ, Chishti AH. BDA-410: a novel synthetic calpain inhibitor active against blood stage malaria. *Mol Biochem Parasitol*. 2007;155:26–32. doi:10.1016/j.molbiopara.2007.05.004

36. Simões AT, Gonçalves N, Nobre RJ, Duarte CB, Pereira de Almeida L. Calpain inhibition reduces ataxin-3 cleavage alleviating neuropathology and motor impairments in mouse models of Machado-Joseph disease. *Hum Mol Genet*. 2014;23:4932–4944. doi:10.1093/hmg/ddu209

37. Nabeshima Y, Washida M, Tamura M, et al. Calpain 1 inhibitor BDA-410 ameliorates a-klotho-deficiency phenotypes resembling human aging-related syndromes. *Sci Rep*. 2014;4:5847. doi:10.1038/srep05847

38. Subramanian V, Uchida HA, Ijaz T, Moorleghen JJ, Howatt DA, Balakrishnan A. Calpain inhibition attenuates angiotensin II-induced abdominal aortic aneurysms and atherosclerosis in low-density lipoprotein receptor-deficient mice. *J Cardiovasc Pharmacol*. 2012;59:66–76. doi:10.1097/FJC.0b013e318235d5ea.

39. Damer CK, Partridge J, Pearson WR, Haystead TA. Rapid identification of protein phosphatase 1-binding proteins by mixed peptide sequencing and data base searching. Characterization of a novel holoenzymic form of protein phosphatase 1. *J Biol Chem*. 1998;273:24396–24405.

40. Grassie ME, Moffat LD, Walsh MP, MacDonald JA. The myosin phosphatase targeting protein (MYPT) family: a regulated mechanism for achieving substrate specificity of the catalytic subunit of protein phosphatase type 1d. *Arch Biochem Biophys*. 2011;510:147–159. doi:10.1016/j.abb.2011.01.018

41. DuVerle DA, Ono Y, Sorimachi H, Mamitsuka H. Calpain cleavage prediction using multiple kernel learning. *PLoS One*. 2011;6:e19035. doi:10.1371/journal.pone.0019035

42. Georgiou DK, Dagnino-Acosta A, Lee CS, et al. Ca^{2+} binding/permeation via calcium channel, CaV1.1, regulates the intracellular distribution of the fatty acid transport protein, CD36, and fatty acid metabolism. *J Biol Chem*. 2015;290:23751–23765. doi:10.1074/jbc.M115.643544

43. Buvinic S, Almarza G, Bustamante M, et al. ATP released by electrical stimuli elicits calcium transients and gene expression in skeletal muscle. *J Biol Chem*. 2009;284:34490–34505. doi:10.1074/jbc.M109.057315

44. Arias-Calderón M, Almarza G, Díaz-Vegas A, et al. Characterization of a multiprotein complex involved in excitation-transcription coupling of skeletal muscle. *Skelet Muscle*. 2016;6:15. doi:10.1186/s13395-016-0087-5

45. Subramanian V, Moorleghen JJ, Balakrishnan A, Howatt DA, Chishti AH, Uchida HA. Calpain-2 compensation promotes angiotensin II-induced ascending and abdominal aortic aneurysms in calpain-1 deficient mice. *PLoS One*. 2013;8:e72214. doi:10.1371/journal.pone.0072214